THE UNIVERSITY OF MICHIGAN

INDUSTRY PROGRAM OF THE COLLEGE OF ENGINEERING

NATURAL CONVECTION FLOW IN LIQUID-METAL MOBILE-FUEL NUCLEAR REACTORS

Frederick G. Hammitt

Associate Professor
Departments of Mechanical and Nuclear Engineering

Elayne M. Brower

Research Associate
University of Michigan Research Institute

December, 1958

IP-340

TABLE OF CONTENTS

LIST OF FIGURES

INTRODUCTION

Various advanced power reactor concepts envision a "mobile-fuel" consisting of a molten alloy, slurry, or solution containing the fissionable material. In fast reactor designs such as LAMPRE-II under development at Los Alamos, the mobile fuel is contained within the core vessel and heat is removed by pumping a coolant through the core, utilizing the core as a conventional closed heat exchanger. It is conceivable that the fuel side of the core be a single, connected vessel with the coolant in separate tubes passing through the core vessel; or that the fuel be contained in separate sealed tubes or ligaments with the coolant on the "shell side". (Figure 1-a and 1-b). A variant is a ligament design with the ligaments connected at one or both ends into headers. (Figure 1-c).

Economic considerations limiting the inactive fissionable material inventory, and requiring maximum utilization of the active inventory result in very small cores, high heat fluxes, and the impossibility of a circulating system. For these reasons, the passage of the coolant through the core rather than the use of an external exchanger seems mandatory for the fast power reactors.

Thermal power reactor concepts such as the LMFR also involve a mobile fuel consisting of fissionable material carried in solution in a molten metal. In this case the core is sufficiently large and the critical loading sufficiently low that a circulating system with external heat exchanger seems most desirable. (Figure 1-d).

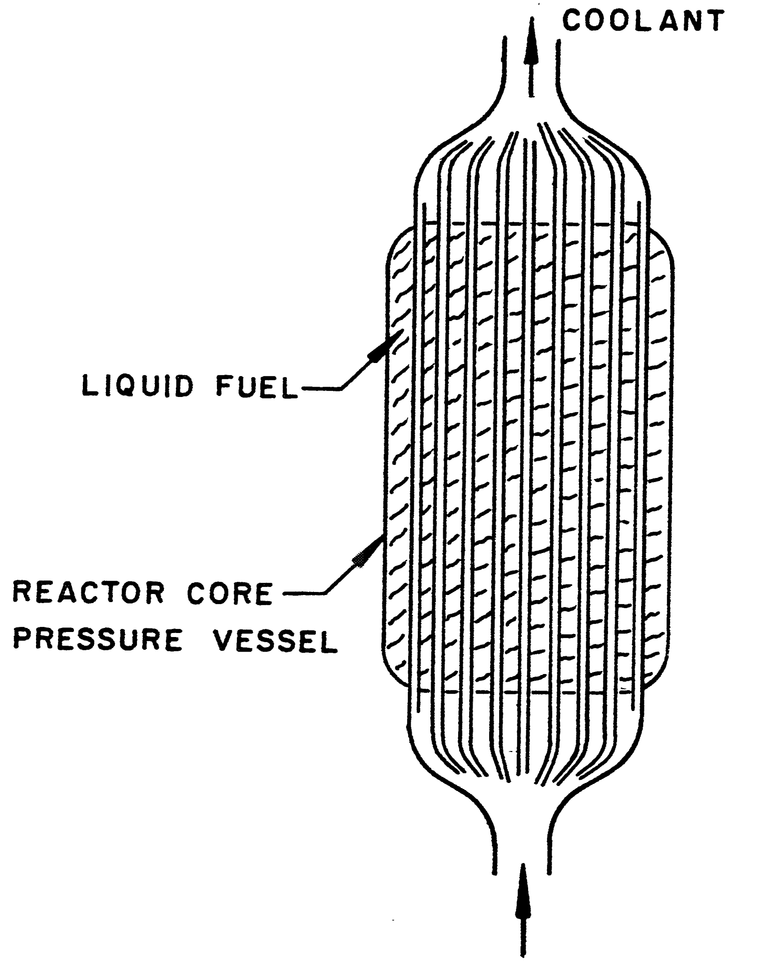

REACTOR WITH COOLANT
FLOW PASSING THRU
TUBES IN THE CORE

FIGURE Ia

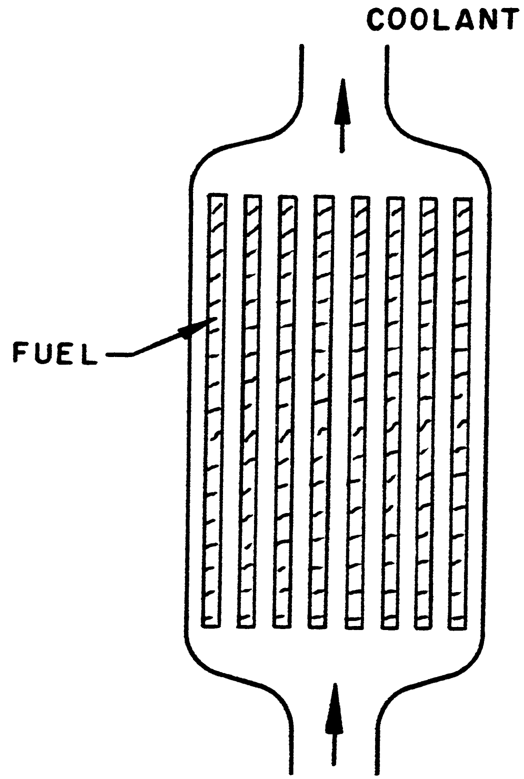

REACTOR WITH FUEL CONTAINED
IN SEPARATE CLOSED TUBES

FIGURE Ib

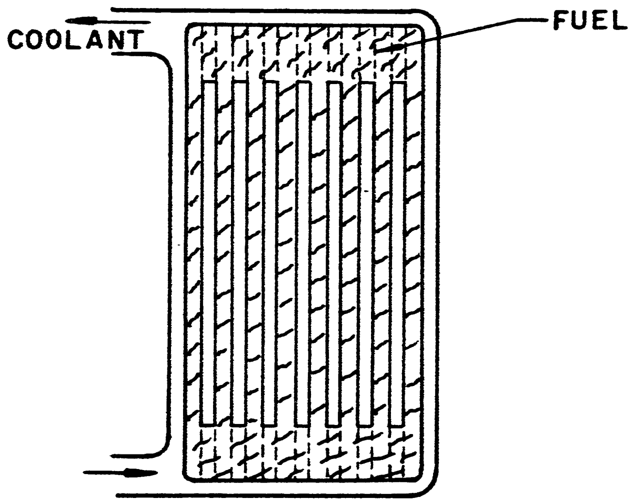

REACTOR WITH FUEL CONTAINED IN SEPARATE TUBES CONNECTED AT TOP AND BOTTOM BY HEADERS

FIGURE 1c

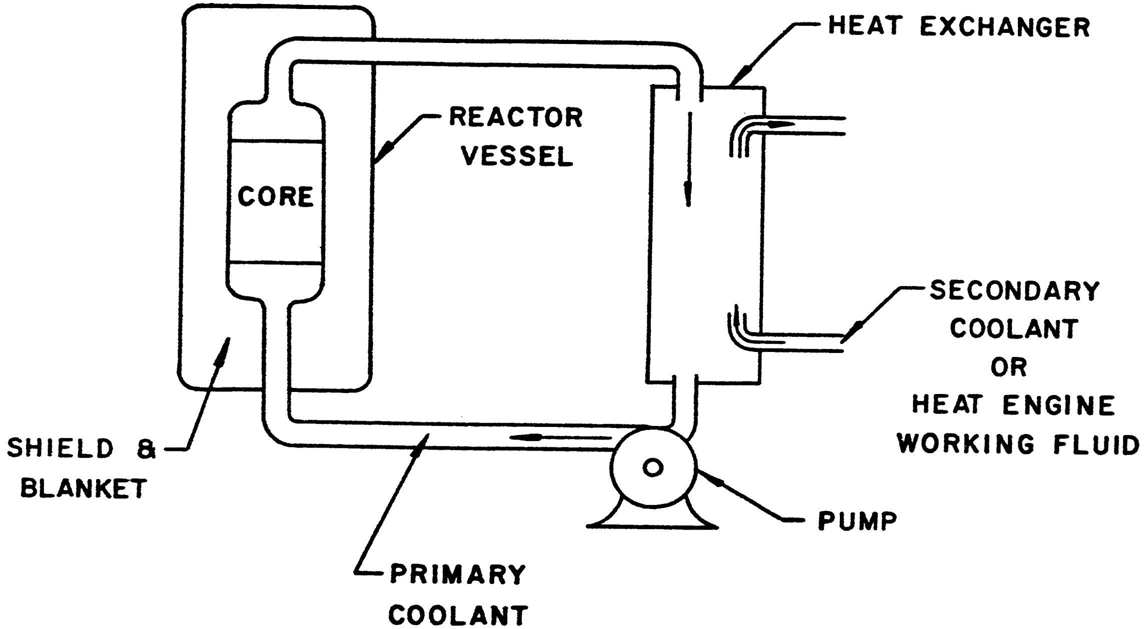

THERMAL REACTOR WITH EXTERNAL HEAT EXCHANGER

FIGURE 1d

In all of these systems natural convective forces influence to a significant extent the velocity and temperature profiles and the heat flux distributions. This is particularly so in the internally cooled cores typical of the fast designs, since no forced convection is superimposed upon the fuel movement. The externally cooled, LMFR-type design exhibits a combined forced-natural convection within the core where the heat is generated and within the fuel cooling in general. This has been treated in Reference 1. The present paper is concerned primarily with the internally-cooled arrangement, where the liquid fuel is within a closed vessel and is motivated by the internal heat generation due to fission and heat loss across the tube walls due to the forced-convection coolant. (Figures 1-a, b, or c).

Limiting the discussion to the internally cooled cores, there are two types of natural convection of interest:

1) The flow and heat transfer within a single, vertical, small-bore ligament (Figure 1-b), in which heat is generated by fission within the fuel and removed to the coolant through the ligament wall;

2) The overall flow and heat transfer within a larger vessel consisting of vertical, parallel, single-ligament passages which are either connected through headers at the ends or continuously connected (Figures 1-a and c).

The flow pattern pertaining to the second configuration is a superposition of the pattern found for a closed-loop with hot and cold leg (Figure 1-d) and that found for a single ligament (item 1 above). The closed loop can be simply approximated if knowledge of the effective friction factor and density change with temperature is available

(Reference 2). This type of behavior would be encountered if the rate of heat generation did not match the coolant flow in a similar manner at all radii (from core centerline). The case of the single, sealed ligament is more difficult to evaluate and will be the primary subject of this paper.

In typical cases involving liquid metals the passage diameters may be very small (perhaps of the order of 50 mils). Although the volumetric heat source is very great, it will often be found that the temperature differences existing between passage centerline and wall are approximately those predicted on the basis of pure conduction; ie, considering the fuel to be a solid rod. Nevertheless, knowledge of the actual temperatures and velocities is important for the following reasons:

1) Actual motion of the fuel (velocities of the order of 100 feet/hour seem typical) even for sealed ligament. Larger values for parallel ligaments may allow mass transport of container material between hot and cold regions.

2) A significant perturbation of the axial distribution of wall heat flux seems probable. Since this is the limiting factor in many designs, realistic knowledge of its magnitude is mandatory.

3) Disposition of the fission gases is affected since the macroscopic velocities are sufficient to overcome the effects of static diffusivity, to affect a hold-up of gas since the velocities are of the magnitude of the rising velocity of small bubbles, and perhaps to affect the bubble growth on ligament walls.

4) If somewhat larger passage diameters are involved, there is a significant effect upon the temperature distributions. The parameter

delineating the effectiveness of the natural convection involves the sixth power of the diameter. Thus small increases in diameter rapidly become of importance.

LIMITING CASES

No analytical or experimental data is presently available for the case of interest; ie, a liquid metal, contained within a vertical, sealed ligament of arbitrary length to diameter ratio within which heat is generated (steady-state being maintained by the removal of this heat through the ligament walls to a coolant), and the walls maintained at arbitrary axial temperature distribution. However, certain limiting cases have been explored both experimentally and analytically and serve to provide a guide for the understanding of the more general case.

A. Boundary Layer Solutions - Aqueous Fluids

Analytical predictions and experimental corroboration for the temperature and velocity profiles for the identical case except that fluids of Prandtl Number of unity or greater were considered, (liquid metal Prandtl Numbers range from perhaps 0.001 to 0.01*) have been detailed in previous papers by one of the present authors (References 3 and 4). The effect of the low ratio of momentum to thermal diffusivities of the liquid metals in general would be to reduce the temperature differentials and velocities.

The flow pattern and temperature profiles, found both experimentally and analytically for the aqueous fluids, are illustrated schematically in Figure 2 (taken from Reference 4). In general there is a rising core of fluid along the centerline which has approximately constant

*It was shown in Reference 5 that the assumptions are not justified for Prandtl Number below about 0.5.

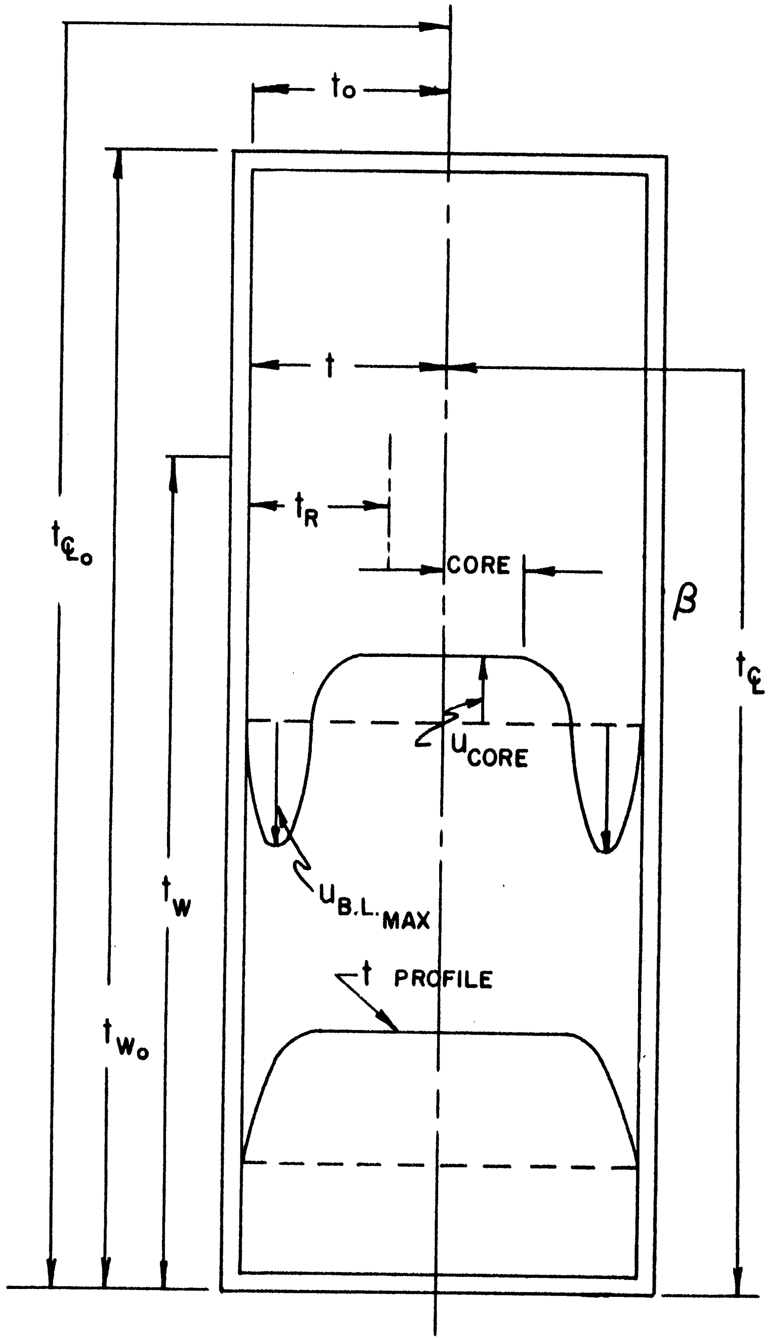

Figure 2. Test Section Nomenclature Schematic.

temperature and velocity at a given axial position. Along the ligament walls there is falling boundary layer wherein the temperature and velocity both vary rapidly as a function of radius. The temperature difference between wall and centerline is a maximum at the top and falls to approximately zero at the bottom. The boundary layer thickness generally grows as the distance from the top increases (behavior typical of any boundary layer) to a maximum near the bottom before, theoretically, becoming abruptly zero at the bottom. As a result of these temperature and boundary layer thickness variations, the wall heat flux is a maximum at the top even though the rate of heat generation for the vessel and the wall temperature is constant. Typical wall heat flux distributions are shown in Figure 3 (taken from Reference 4).

It was found that the overall temperature differences could best be presented in a plot of non-dimentional volumetric heat source versus non-dimensional temperature differential. Such a plot, taken from Reference 4 is included (Figure 4) for convenience. The various curves apply to different wall temperature distributions (all linear in the axial direction and uniform around the circumference at each axial position) and axial heat source distributions (no variation of heat source with radius was considered). Because of presentation in non-dimensional parameters, the results are applicable to any length to diameter ratio. The meaning of the symbols is given in the Nomenclature and on Figure 2.

It is noted from Figure 4 that the lines terminate, depending upon wall temperature distribution, at a q_V between 10^2 and 10^3. This termination signifies the lower limit of applicability of the boundary layer solution used. At this q_V value the boundary layer, at some point

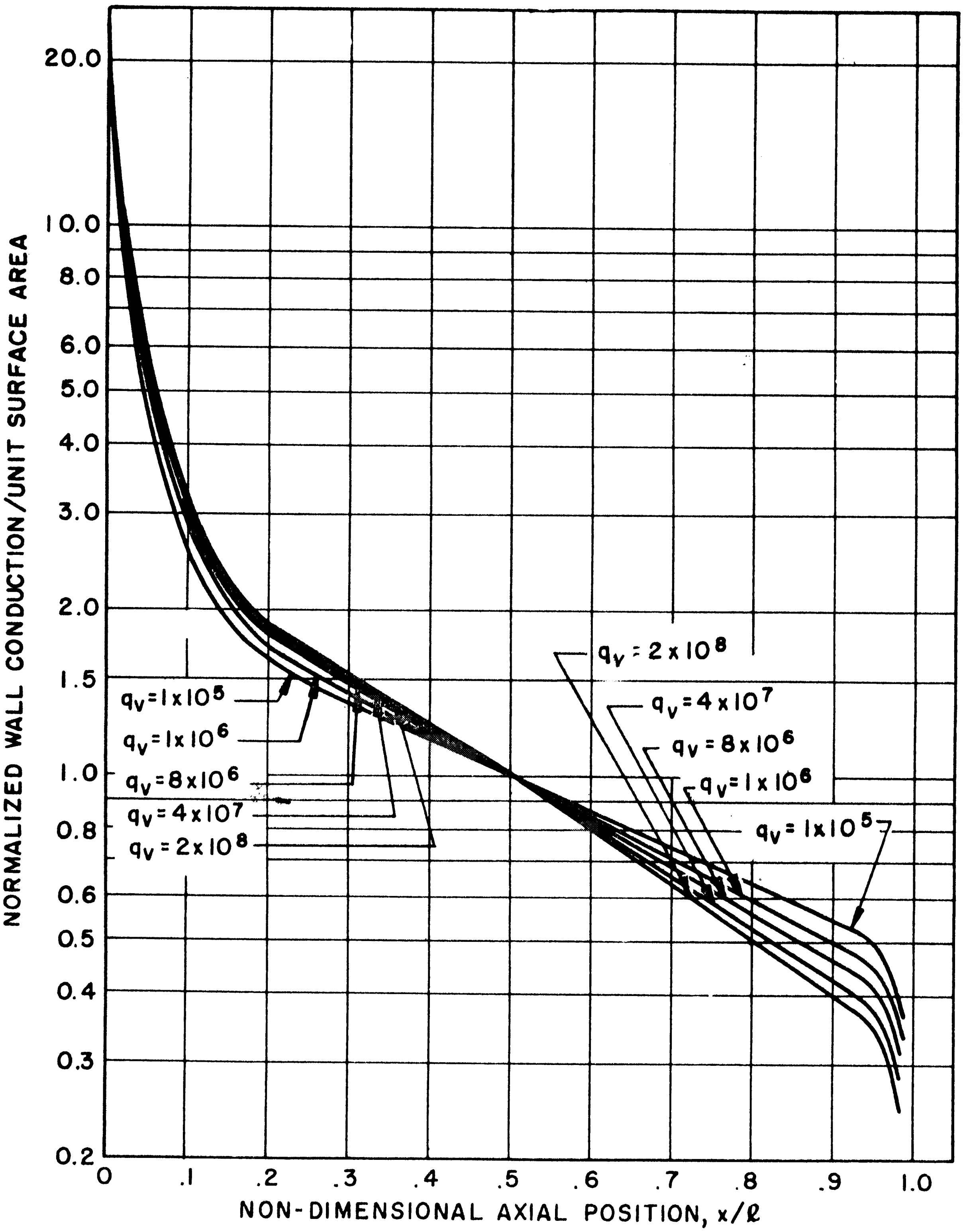

Figure 3. Normalized Wall Conduction vs. Non-Dimensional Axial Position, Constant Wall Temperature, Uniform Heat Source Distribution.

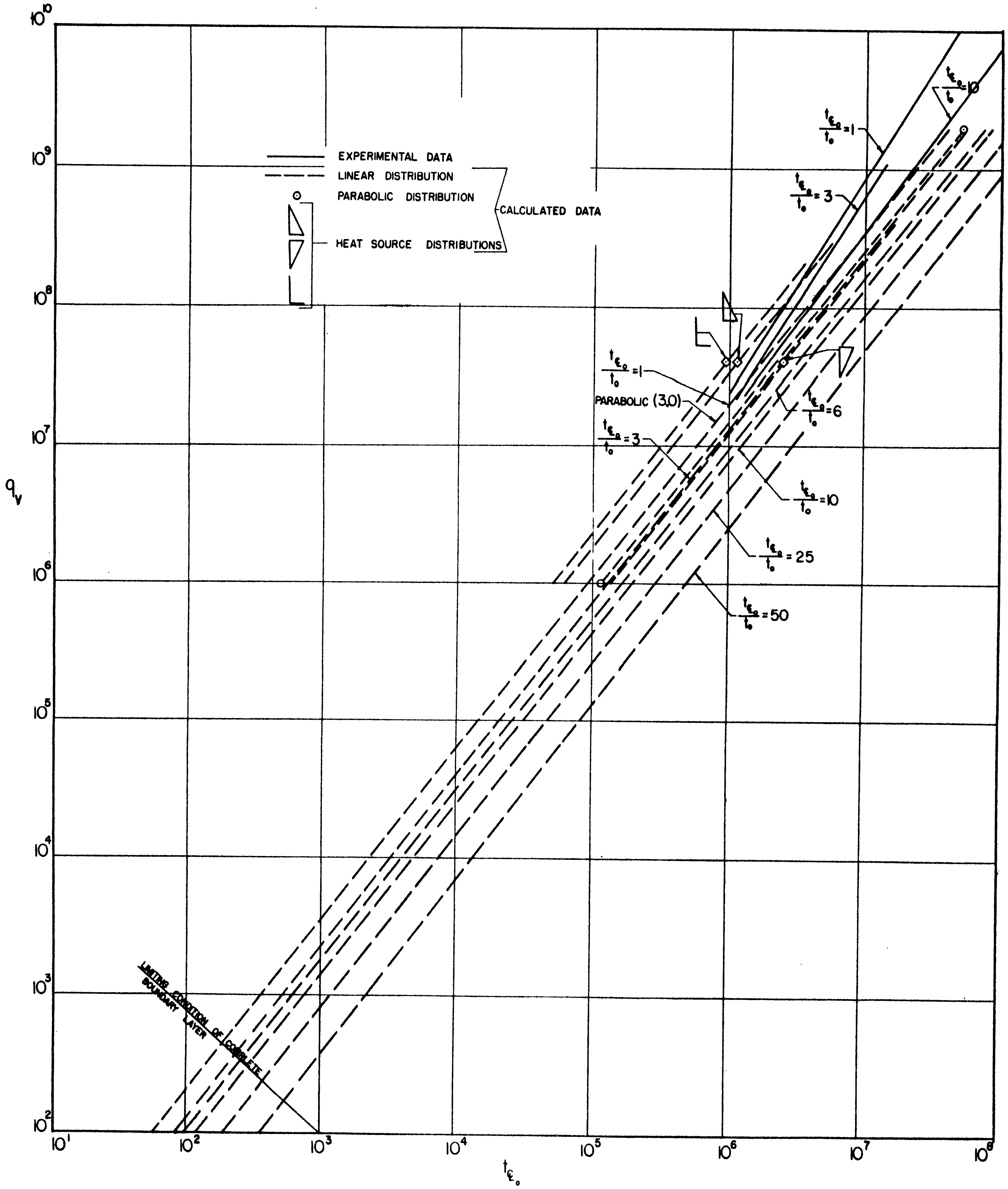

Figure 4. **Non-Dimensional Heat Source vs. Overall Temperature Differential, Experimental and Calculated Data.**

along the axis, has grown to the extent of filling the entire vessel (as here used, the boundary layer includes some upward velocity region, see Figure 2, so that continuity is not disregarded). The solution was based upon the requirements of conservation of mass, energy, and momentum, and then the substitution of assumed temperature and velocity profiles of the type shown in Figure 2, with boundary layer thickness a function of axial position. Once the boundary layer has grown to the extent of filling the entire vessel, it is obvious that the assumed profiles, allowing a core of uniform temperature and velocity, no longer apply, and that the boundary layer thickness can no longer be a function of axial position. Calculation of typical cases show that the region of interest for liquid-metal mobile-fueled fast reactors is usually in this region of q_V, ie, below 10^2. However, the significance of such a q_V is not known since the analysis is limited to higher Prandtl Numbers.

If a completely similar analysis is followed except that the boundary layer thickness is fixed equal to the vessel radius, a difference equation relating the non-dimensional temperature differentials, heat source, and axial position can be derived. The steps in addition to the analysis of Reference 2 are shown in the appendix. A typical plot of non-dimensional temperature difference between centerline and wall as a function of axial position is shown in Figure 5 for various heat source strengths at constant temperature. If a variable wall temperature is assumed, the temperature differential in the center section will be unchanged and the top and bottom will be changed only slightly from the constant wall temperature case. It is noted that the temperature differential starts at zero at the bottom and becomes assymptotic to $q_V/4$,

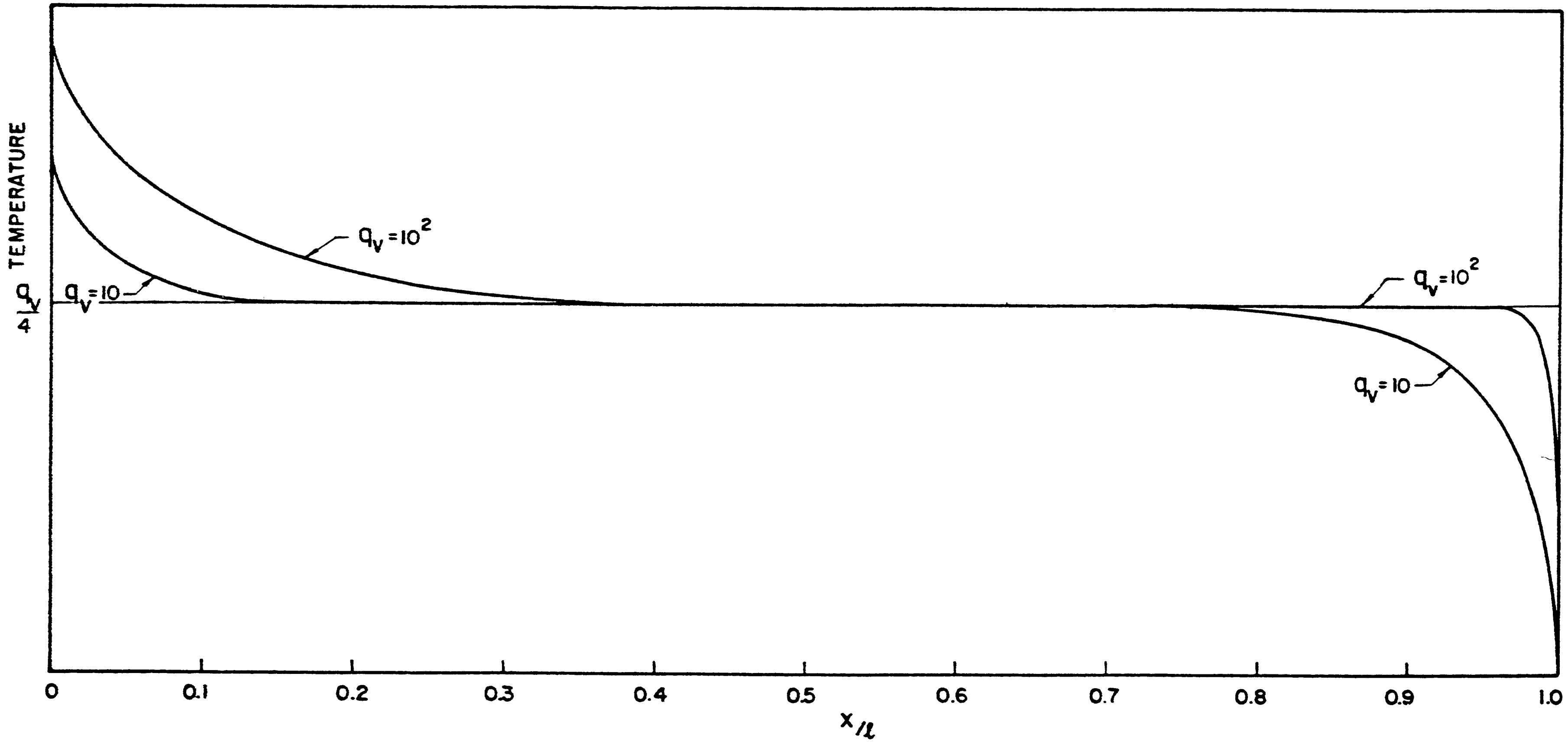

Figure 5. Temperature vs. Axial Position, Constant Wall Temperature

approaching this value very rapidly for small q_v. This analysis, like the original of Reference 3, is limited to Prandtl Number near unity. This value of the non-dimensional temperature differential corresponds to the case of static conduction.

For those cases where the non-dimensional heat source is sufficiently low so that the boundary fills the entire vessel at some point, it is necessary to use a combined solution. The original solution of reference 3 can be used for that portion of the vessel near the top where the boundary layer is growing. The "fully-developed" solution (boundary layer thickness equal to radius and constant) can then be used for the remainder of the vessel. Such a combination will assure that conservation of mass, momentum, and energy are observed for any radial plane through the vessel at any axial position. To assure consistency at the point of joining of the solutions it is necessary that the original boundary layer solution give a temperature differential of $q_v/4$ at the axial position where the boundary layer thickness becomes equal to the vessel radius. As pointed out in Reference 3, the implementation of the boundary layer solution involves a numerical procedure with an IBM-650 program.

It may be noted that the situation is somewhat analogous to that of pipe flow where the boundary layer grows in the entry section (analogous to the ligament top) until it occupies the entire pipe. Henceforth it is "fully-developed" and no longer grows with axial distance.

B. Infinite Length/Diameter Case - Aqueous or Liquid Metal

At the opposite extreme from the boundary layer case explored in Reference 4, where effectively the length to diameter ratio was sufficiently small that the temperature and velocity gradients were limited only to the vicinity of the wall and the boundary layer effects could not extend into the central portion before reaching the bottom of the tube, is the case of infinite length to diameter ratio. An examination of the parameter grouping which forms q_V discloses that this corresponds to zero non-dimensional heat source. The infinite length case has been examined in detail by Murgatroyd, Reference 6. A short examination of the physical situation will disclose the significant features.

If the flow is laminar and the tube infinitely long, it is obvious that transfer of heat normal to the axis can be accomplished only by conduction. There are no convective effects either from turbulent mixing or transport of ascending fluid along the centerline to descending fluid along the wall at the ends (since they are infinitely distant). This is the case of "rod flow" for which the Nusselt's Number based on diameter and mixed mean temperature is 8 (Reference 7). It is shown in the appendix to this paper that such a Nusselt's Number corresponds to a non-dimensional temperature differential between wall and centerline equal to $q_V/4$ at a given axial position. As previously mentioned the fully-developed solution was asymptotic to this value for low q_V. We have thus an independent verification of this solution.

It should be mentioned that the assumption of laminar flow is well justified for the fast reactor applications. As mentioned in Reference 4, the transition from a generally laminar condition to a generally turbulent one appears to occur at a Rayleigh Number based on vessel radius of about 4×10^7. This roughly corresponded to q_V of about 10^8 for the tests conducted. The corresponding Rayleigh Number and q_v for a typical fast reactor application are about 50 and 10.

C. Effect of Liquid Metals as Compared with Aqueous Fluids

No analysis or experiment applicable to the boundary layer regime has been made for fluids with low Prandtl Number in the applicable geometry. However, the infinite length analysis applies regardless of Prandtl Number. It seems certain that the general type of flow behavior observed and predicted for aqueous fluids with high q_V would also be observed with liquid metals. However, the low Prandtl Number should result in the temperature differences for a given heat source being reduced and the temperature gradients extending further into the fluid. Since the temperature differences would be less, the coefficient of volumetric expansion is generally small, and the conductivity large, the Rayleigh Numbers would be much lower, the forces motivating natural convection circulation less, and the velocities probably reduced. Nevertheless, the asymptote reached as q_V approaches zero is the same. On the basis of these qualitative considerations, it seems likely that the general type of behavior would be the same, but that the fully-developed flow condition would be reached at a somewhat higher q_V since the temperature gradients should extend more deeply into the fluid.

APPLICATION OF RESULTS TO SMALL-BORE LIGAMENT WITH LIQUID METALS

Utilizing the limiting results discussed in the previous section, it is possible to delineate the significant results to be expected from natural convection in a small-bore ligament filled with liquid metal fuel in a typical fast power reactor design.

A. Temperature Differentials - Centerline to Wall.

The results for aqueous fluids within the range of the boundary layer solution (q_V above about 10^3) are shown in detail in References 3, 4, 8 and 9. These are not directly applicable to liquid metals but the type of behavior for high q_V is probably typical. However, the cases of interest to the liquid metal fast reactor concepts which have come to the attention of the authors, show q_V values within the fully-developed range. Figure 5 shows the non-dimensional temperature differential (in units of $q_V/4$) as a function of axial position and q_V for constant wall temperature. The significant results are listed in Table I. It is noted that the temperature differential is equal to approximately $q_V/4$ for most of the vessel length but shows an increase near the top and a decrease at the bottom. The degree of increase at the top is a function of q_V but is a maximum of about 70% of $q_V/4$ at $q_V = 10^2$. This is also very local (occurring within 6% of the top) and may not be of any real significance since small axial heat flow in the tube wall could relieve over-heating. As far as the central portion of the tube is concerned the results apply directly to any axial wall temperature distribution so long as the axial gradient is not so great that axial conduction of heat becomes significant compared with radial.

The results at the tube ends apply strictly only to constant wall temperature. However, they are typical of any distribution since the substitution of different temperature configurations produces differences only of degree. Also, the end results apply only to aqueous fluids, while the central portion is of general applicability. However, it is believed that fluids of low Prandtl Number would exhibit similar behavior, although the end effects would be somewhat reduced in magnitude and axial extent.

B. Wall Heat Flux

The axial wall flux distribution for uniform heat source, constant wall temperature, and aqueous fluids for the fully-developed condition is shown in Figure 6 and listed in Table I. Figure 3 showed similar results for the boundary layer solution at high q_V but included the effects of wall temperature distribution. In both cases it is noted that there is a decrease of wall heat flux at the bottom, a generally constant region in the central portion, and a sharp rise toward the top. These effects become very much more localized as q_V is reduced into the fully-developed region of interest in the present application. As in the case of temperature differential, the central portion of the curves are applicable for any fluid and wall temperature distribution, again with the qualification that the axial gradients cannot be so sharp that axial conduction becomes relatively large. The end portions apply strictly to aqueous fluids and constant wall temperature. However, a local rise of somewhat similar magnitude is to be expected with liquid metals and various wall temperature distributions. As in the case of the temperature rise at the top, this increase of heat flux may not be physically significant because of its very local character. Local over-

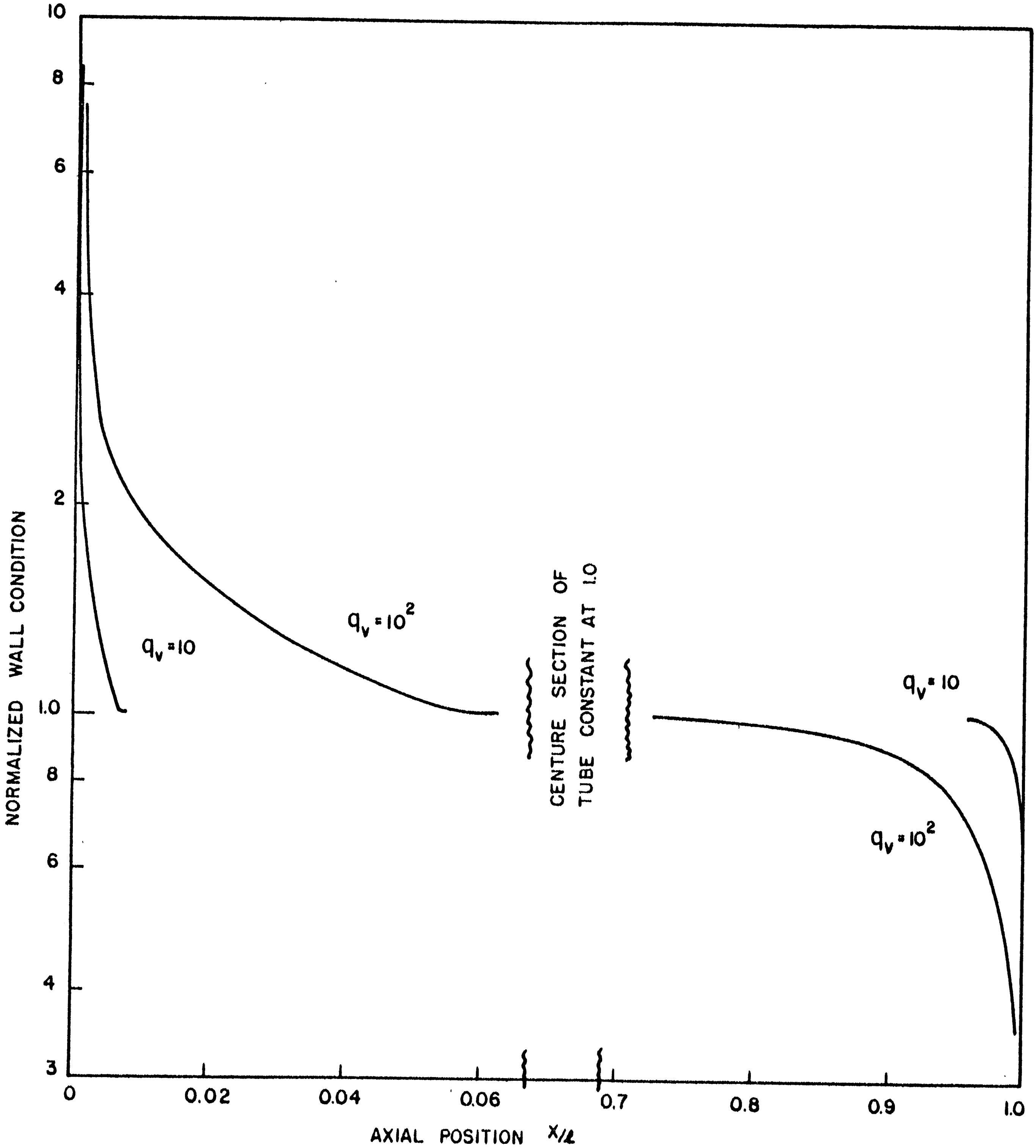

Figure 6. Normalized Wall Conduction for Constant Wall Temperature and Uniform Heat Generation - Fully Developed Flow

heating encountered in this respect may well be relieved by axial heat flow. Only experimental results could resolve the seriousness of the problem. The problem is of potential importance because the thermal stresses due to the wall heat flux are the limiting factor in many designs.

C. Velocity

Detailed plots of the velocities anticipated and also observed for aqueous fluids in the boundary layer regime are given in references 3, 4, 8, and 9. Reference 6 shows analytical predictions for laminar and turbulent flow in vessels of infinite length. Figure 7 shows the maximum velocity to be expected in the laminar fully-developed regime as a function of axial position and q_v. As previously mentioned, the physical cases of interest seem limited to laminar flow. Except for the extreme ends, the values apply to any fluid and any wall temperature distribution. Also the end values should be correct in direction of shift and order of magnitude. Under the assumed profiles used in this solution (a quadratic curve was used) the maximum velocity is the ascending velocity along the centerline although in the high q_v boundary layer cases it was the descending velocity adjacent to the wall. Whether the prediction of maximum velocity along the centerline is justified or is merely a result of the assumptions used is not known. However, the order of magnitudes of velocities predicted is of prime importance and this is believed to be essentially correct.

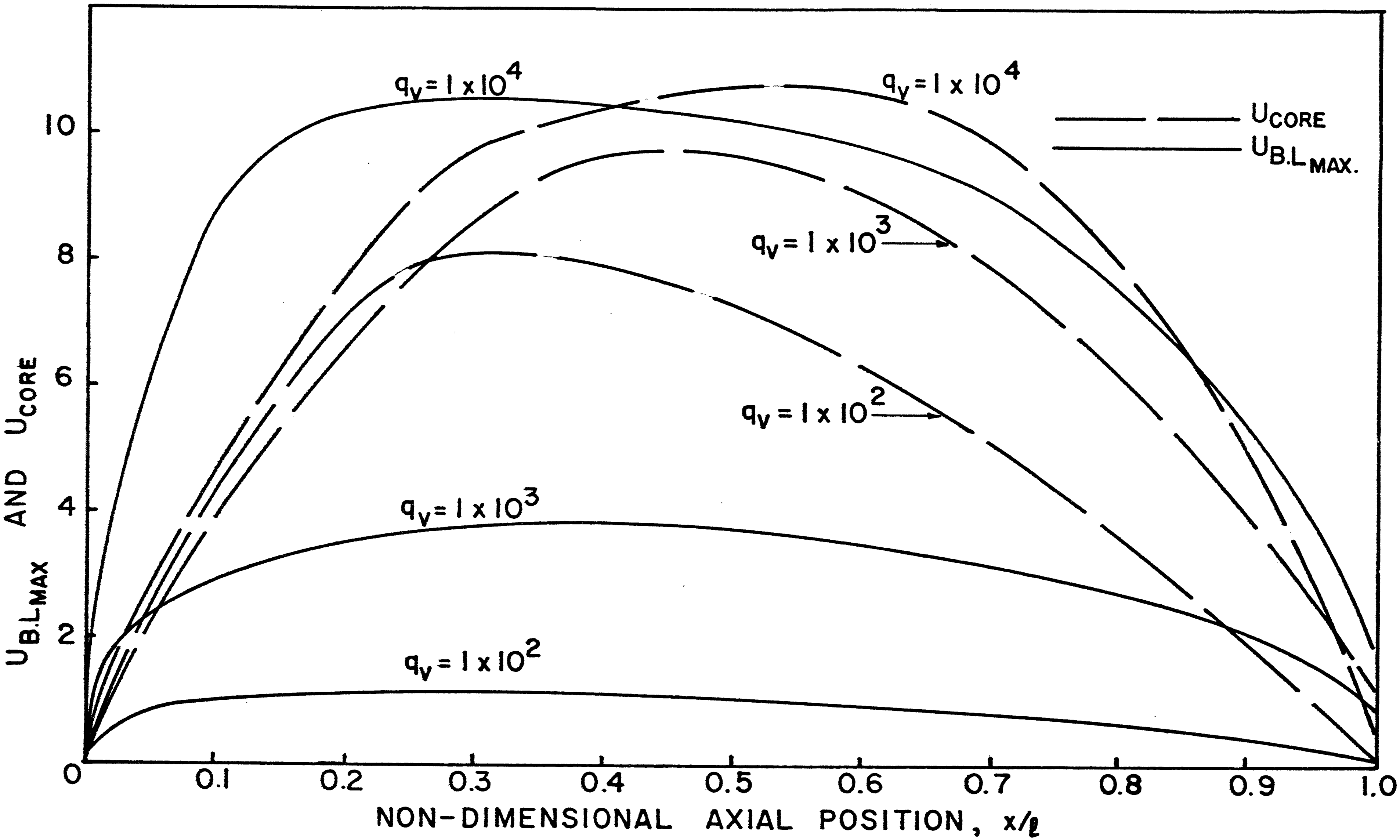

Figure 7. Non-Dimensional Boundary Layer and Core Velocity vs. Axial Position, Constant Wall Temperature

CONCLUSIONS

Although no directly applicable theoretical or experimental results are available for natural convection in single, small-bore vertical liquid-metal filled ligaments as encountered in mobile-fuel fast power reactors, it is possible to delineate the general nature of behavior expected with respect to temperature, velocity, and wall heat flux profiles from limiting analyses and experiments which are available. These data are illustrated in the paper, and it is shown that natural convection may be of importance from the viewpoints of perturbation of wall heat flux (a limiting design condition), and the motivation of velocities important as a possible mechanism for mass transport and also as an influence on the disposition of fission gas created within the fluid.

APPENDIX

Long Tube (Fully-Developed Flow) Analysis

In order that the solutions will be consistent at the transition points, the same arbitrary velocity and temperature profiles are assumed as in Reference 8. However, it is assumed that the boundary layer thickness is no longer a function of x but is constant and equal to the tube radius.

From Reference 8

$$t = t\ [1 - (\frac{r - \beta}{1 - \beta})^2] \tag{1}$$

$$u = -\gamma[1 - (\frac{r - \beta}{1 - \beta})^2 \{1 + \delta(r - 1)\}] \tag{2}$$

but $\beta = 0$, therefore

$$t = t\ (1 - r^2) \tag{3}$$

$$u = -\gamma\ [1 - r^2(1 + \delta\{r - 1\})] \tag{4}$$

Substituting equation (4) into the continuity relation (Reference 8)

$$\int_0^1 r\ u\ dr = 0 = -\gamma\ \{\int_0^1 r\ dr - \int_0^1 r^3\ dr - \delta\int_0^1 r^4\ dr + \delta\int_0^1 r^3\ dr \tag{5}$$

from which $\delta = -5$. Equation (4) can then be written as

$$u = -\gamma(5r^3 - 6r^2 + 1) \tag{6}$$

and at $r = 0$, $\frac{du}{dr} = -\gamma(15\ r^2 - 12r) = 0$ (7)

Now, substituting the velocity and temperature profiles, Equations (3) and (4) into the momentum equation (Reference 8)

$$-\int_0^1 r\ t\ dr + \frac{1}{2}\ (t)_{r=0} + \left(\frac{\partial u}{\partial r}\right)_{r=1} = 0 \tag{8}$$

we get $\gamma = \frac{t}{12}$ and (9)

the velocity, Equation (6) becomes

$$u = -\frac{t}{12}\ (5r^3 - 6r^2 + 1) \tag{10}$$

Repeating the same procedure with the integrated energy equation (Reference 8)

$$\frac{\partial}{\partial x}\int_0^1 r\ u\ t\ dr = \left(\frac{\partial t}{\partial r}\right)_{r=1} - \frac{q_v}{2} \tag{11}$$

we have $\frac{\partial}{\partial x}\int_0^1 r\ u\ t\ dr = -\frac{1}{336}\frac{\partial}{\partial x}\ (t^2)$ (12)

$$\left(\frac{\partial t}{\partial r}\right)_{r=1} = -2t \tag{13}$$

and Equation (11) reduces to

$$\underbrace{-\frac{1}{336}\ \frac{\partial}{\partial t}\ (t^2)}_{\text{axial convection}} + \underbrace{2t}_{\text{wall conduction}} + \underbrace{\frac{q_v}{2}}_{\text{heat source}} = 0 \tag{14}$$

From Equation (14) it can be seen that t approaches $q_v/4$ as a limit as the tube length becomes infinite ($\partial/\partial x \rightarrow 0$). The axial convection term is a function of the axial temperature and the wall conduction term is a function of the wall to centerline differential temperature. Hence

$$-\frac{1}{336}\frac{\partial}{\partial x}\, t_{\mathbb{C}}^{2} + 2t + \frac{q_v}{2} = 0 \qquad (15)$$

where $t_{\mathbb{C}} = t + t_w$

Therefore

$$-\frac{(t + t_w)_N^{2} - (t + t_w)_{N-1}^{2}}{\Delta x} + 672t + 168q_v = 0 \qquad (17)$$

and

$$t_{N-1} = -(t_{w_{N-1}} + 168\Delta x) +$$

$$\sqrt{(t_{w_{N-1}} + 168\Delta x)^2 + (t_N + t_{w_N})^2 - 336\Delta x t_N + 168 q_v \Delta x - t_{w_{N-1}}^{2}} \qquad (18)$$

where Δx and t are positive numbers.

Natural Convection Laminar Flow in Infinate Length Tube

The heat flow in the axial direction must be negligible compared with flow in the radial direction for the case of pure conduction, and the heat lost through the wall in a given axial section must equal the heat generated in that section.

Then $T = -\frac{Q_v r^2}{4k} + C_1 \ln r + C_2$ (Reference 2, page 662)

$$T_{\mathbb{C}} - T = \frac{Q_v}{4k}(R^2 - r^2)$$

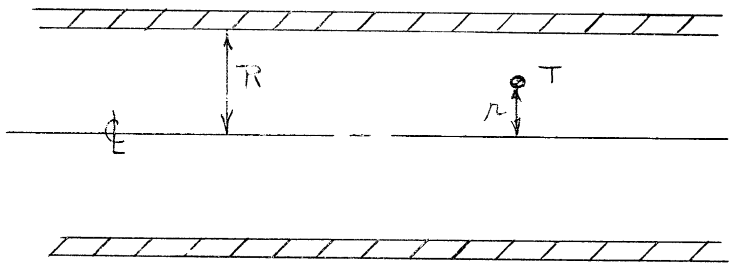

$$T = T_{\text{℄}} - \frac{Q_V}{4k}(R^2 - r^2)$$

$$T_{mean} = \frac{\int T\, dv}{v} = \frac{L\int_0^R T_{\text{℄}} - \frac{Q_V}{4k}(R^2 - r^2) 2\pi\, r\, dr}{L\pi R^2}$$

$$= T_{\text{℄}} - \frac{Q_V}{8k} R^2 = T_{\text{℄}} - \frac{h_{\text{℄}} R(T_{\text{℄}} - T_W)}{4k}$$

$$h_{\text{℄}} = \frac{Q_{wall}}{A_{wall}(T_{\text{℄}} - T_W)} = \frac{Q_V\, \pi R^2 L}{2\pi RL(T_{\text{℄}} - T_W)} = \frac{RQ_V}{2(T_{\text{℄}} - T_W)}$$

$$Q_V = \frac{2h_{\text{℄}}\, T_{\text{℄}} - T_W}{R}$$

but previously $T_{\text{℄}} - T_W = \frac{Q_V}{4k} R^2$

so $T_{\text{℄}} - T_W = \frac{2h_{\text{℄}}\,(T_{\text{℄}} - T_W)R^2}{4k\, R} = \frac{h\, R}{2k}(T_{\text{℄}} - T_W)$

and $h_{\text{℄}} = \frac{2k}{R}$ for pure conduction

$$T_{mean} = \frac{T_{\text{℄}} + T_W}{2}$$

McAdams, Reference 7, page 233, shows that for an infinately long tube with laminar (rod-like flow) and uniform heat flux the Nusselt's

Number based on the diameter and the mean temperature is 8 away from the entrance section.

$$Nu_{D,T_{mean}} = \frac{h\ D}{k} = 8 \quad \text{or} \quad Nu_{a,T_{mean}} = \frac{h\ a}{k} = 4$$

Thus, based on the radius and the temperature difference from wall to centerline

$$Nu_{a,T_{℄} - T_W} = 2$$

In the present analysis using the non-dimensional heat source term, q_v,

$$Nu_{a,T_{℄} - T_W} = \frac{q_v}{2t}$$

by simple algebraic substitution for q_v and t in terms of the physical quantities. And when $t = q_v/4$

$$Nu_{a,T_{℄} - T_W} = \frac{q_v}{2t} = \frac{q_v}{2\ \frac{q_v}{4}} = 2$$

NOMENCLATURE

a	Radius of test section
c_v	Specific heat
g	Acceleration of gravity
h	Film coefficient for heat transfer
k	Thermal conductivity
ℓ	Length of test section
Nu_a	Nusselt's Number based on radius; $\frac{ha}{k}$
Pr	Prandtl Number; $\frac{\nu}{\kappa}$
q_v	Non-dimensional volumetric heat source $\frac{Q_v a^6 \alpha g}{\rho^2 \kappa^2 \ell c_v}$
Q_v	Volumetric heat source -- energy per unit volume
Ra_a	Rayleigh Number based on radius and maximum temperature differential; $\frac{\alpha g a^3 (\Delta T_{Max_{℄ \text{ to Wall}}})}{\nu \kappa}$
Ra_ℓ	Rayleigh Number based on length and maximum temperature differential; $\frac{\alpha g \ell^3 (T_{Max_{℄ \text{ to wall}}})}{\nu \kappa}$
R, r	Dimensional and non-dimensional coordinates in radial direction
T	Temperature
t	Non-dimensional temperature differential $= \frac{\alpha g a^4 \Delta T}{\nu \kappa \ell}$; without subscript non-dimensional temperature differential wall and fluid at any given axial position. Subscript o applies to top of tube centerline. Subscript ℄ applies to centerline. $Nu_a = q_v / 2t_{℄_o}$.
U	Velocity in axial direction
u	Non-dimensional velocity in axial direction $= a^2 U / \kappa \ell$
v	Volume

NOMENCLATURE (CONT'D)

X,x	Dimensional and non-dimensional coordinates in axial direction
α	Coefficient of volumetric expansion
β	Non-dimensional core thickness. $1 - \beta$ is non-dimensional boundary layer thickness.
κ	Thermal diffusivity $= k/\rho c_v$
ν	Kinematic viscosity
ρ	Density

BIBLIOGRAPHY

1. Poppendiek, H.F., and Palmer, L.D., "Heat Transfer in Heterogeneous Circulating-Fuel Reactors," Nuclear Science & Engineering, Vol. 3, No. 1, January 1958.

2. Glasstone, S., "Principles of Nuclear Reactor Engineering," Van Nostrand Co. Inc., New York, 1955

3. Hammitt, F.G., "Modified Boundary Layer Type Solution for Free Convection Flow in Vertical Closed Tube with Arbitrary Distributed Internal Heat Source and Wall Temperature," ASME paper number 58-SA-30, Semi-Annual Meeting, Detroit, Michigan, June 15-19, 1958.

4. Hammitt, F.G., "Natural Convection Heat Transfer in Closed Vessels with Internal Heat Sources - Analytical and Experimental Study," to be presented at ASME Annual Meeting, New York, Nov. 30 - Dec. 5, 1958.

5. Mohr, Dale, "Evaluation of the Prandtl Number Error in the Modified Boundary Layer Type Solution for Free Convection Flow in Vertical Closed Tube with Arbitrarily Distributed Internal Heat Source and Wall Temperature," Master's Thesis in Nuclear Engineering, University of Michigan, Ann Arbor, Michigan, June, 1958.

6. Murgatroyd, W., "Thermal Convection in a Long Cell Containing a Heat Generating Fluid," AERE ED/R 1559, Harwell, 1958.

7. McAdams, W.H., "Heat Transmission," McGraw-Hill Book Company, New York, 1954.

8. Hammitt, F.G., "Heat and Mass Transfer in Closed, Vertical, Cylindrical Vessels with Internal Heat Sources for Homogeneous Nuclear Reactors," Ph.D. Thesis, University of Michigan, Ann Arbor, Michigan, February 1958.

9. Brower, E.M., "Heat and Mass Transfer in Closed Cylindrical Passage of Homogeneous Nuclear Reactors with Internal Heat Generation," Master's Thesis in Nuclear Engineering, University of Michigan, Ann Arbor, Michigan, June 1958.